Numerical Modelling and Optimization of Thermal Performance of Heat Sink with Uniform Cross - Sectional Area using Shape Optimized Al$_2$O$_3$ - SiC Nanoparticles in Base Fluid

Ammembal Gopalkrishna Pai[1], Rekha Gopalkrishna Pai[2,*], Abdullah Abdul Samat[3], Akshatha Bekal Laxmish[4]

[1] Department of ECE, Manipal Institute of Technology, Manipal Academy of Higher Education, Manipal, Karnataka, 576104, India
[2] Department of Mathematics, Manipal Institute of Technology, Manipal Academy of Higher Education, Manipal, Karnataka, 576104, India
[3] Department of Mechanical Engineering, Universiti Malaysia Perlis, Pauh Putra Campus, 02600 Arau, Perlis, Malaysia
[4] Department of Mathematics, Manipal Institute of Technology, Manipal Academy of Higher education, Manipal, Karnataka, 576104, India

ARTICLE INFO	ABSTRACT
	This study explores the flow characteristics of proposed "*Integrated hybrid nanofluid heat sink model (IHNFHSM)*" with a novel mixture of Al$_2$O$_3$–SiC nanoparticles of various shape in base fluid. The primary objective is to evaluate the influence of various similarity parameters on the heat transfer performance of the fin structure subjected to convective and insulated tip boundary conditions. A novel combination of Al$_2$O$_3$–SiC hybrid nanoparticles offer a significant potential for improved dissipation of heat in engineering applications. The analysis is carried out using Darcy's model, incorporating temperature-dependent natural convection, and radiation effects. The governing energy equations are non - dimensionalized and solved using *three stage Lobatto quadrature* numerical technique with suitable boundary conditions. The results provide insight into the effect of similarity parameters on the thermal performance of the system under consideration. Quantitatively, the findings reveal an increase of 23% in the thermal conductivity of base fluid with hybrid nanoparticles. The heat transfer rate of convective fin tip was enhanced by an average of 17.13% at $Nc = Nr = m_2 = 1$ compared to an insulated fin tip. An optimal thermal performance of the model in terms of heat transfer rate was observed by an enhancement of 100% in Nc, Nr and m_2 values from 10 to 20. Additionally, dimensionless fin temperature at Nc = 1 enhanced by 12.16% for the lamina – lamina shape combination of nanoparticles over lamina – spherical, clearly showing its dominance in the thermal performance over the rest of the combinations.

1. Introduction

In thermal engineering, the fundamental principle to enhance the heat transfer rate is to make use of an extended surface known as a fin. Thermal management is a primary concern in many of the engineering applications, especially in electronics, automotive industries and energy, where heat

---

dissipation requirement is high for reliability and optimal performance. It is seen that the conventional cooling methods often fail in meeting the requirements for efficient heat dissipation, leading the researchers to explore the advanced cooling system that involves nanofluids. Nanofluids, especially hybrid nanofluids offers very high thermal conductivity that could lead to more effective cooling systems. The shape and dimensions of the fin also plays a major role in the design to improve the heat transfer efficiency of the system under consideration. Optimizing the design parameters to improve the thermal performance of the system is a major challenge for researchers. Thus, it becomes essential to come up with a system that can enhance the heat transfer rate in an efficient and effective manner.

The effectiveness of straight fins under heat and mass transfer was investigated Sharqawy and Zubair [1]. The result shows that efficiency of the fin improves with the rise in air pressure. The behavior of exponential fin was examined by Din *et al.,* [2]. An improvement in heat transfer was observed in the exponential fin compared to the trapezoidal fin. The problem was numerically solved using the shooting technique. Turkyilmazoglu [3] proposed an optimization in the fin dimension by considering concave–parabolic fin geometry in the analysis. Kezzar *et al.,* [4] conducted a study on heat transmission within a convective fin of different shapes, considering various factors such as internal heat generation, variable thermal conductivity, and radiation. The investigation showed the superior performance of the exponential fin over the other profiles. Hosseinzadeh *et al.,* [5] experimentally verified the triplex tube heat exchanger incorporating tree-like fins under the influence of fluid containing MoS_2 and TiO_2 nanoparticles. The analysis was performed using the GFEM method, which indicates the outperformance of the tree-like fins, as it considerably reduces the solidification time. Numerical investigation on rectangular LHSU with melted P116 parafin wax in aluminium trioxide nanoparticles was carried out Elbahjaoui and Qarnia [6]. Ahmad *et al.,* [7] examined the thermal profile of longitudinal heat exchangers (fins) of different shapes using complex ordinary differential equations (ODE) with boundary values with an innovative approach termed the ANN-SOS algorithm. The outcomes were verified and agreed with those in the existing literature. An analysis of the thermal performance of a microchannel heat sink with various fin shapes using a numerical technique was conducted by Ali *et al.,* [8]. Zig-zag fin and 3% Al_2O_3 nanofluid combination showed the best thermal performance. Syed *et al.,* [9] came up with an innovative design of DPHE that considerably the friction loss, cost and weight, thus making it more energy efficient. Mukeshkumar and Kumar [10] numerically examined the heat sink wetted with aluminium trioxide water based nanofluid. The structure was simulated using ANSYS software, and the results showed an approximate increase of 60% in the heat-transfer coefficient. An experimental study to analyze the heat transmission characteristics of an MCHS heat sink under the influence of hybrid nanofluids was conducted by Vinoth *et al.,* [11]. An improvement of 3% in the heat transmission rate was observed, thus making it a more efficient medium for power converters in EV. Sowmya *et al.,* [12] investigated the thermal behavior of various fin profiles, assuming a variation in the thickness along its length. The results show a substantial improvement in the thermal efficiency of the rectangular fin and the drop rate in the triangular fin. Nabati *et al.,* [13] used the Sinc collocation method to study the temperature distribution and heat transfer capabilities of porous fins exposed to radiation, magnetic fields, and a porous medium. Atouei *et al.,* [14] investigates the thermal analysis of semi-spherical fins with heat generation, radiation, and temperature-dependent properties using least square and collocation methods, validating the analytical solutions with numerical results and demonstrating the effectiveness and accuracy of these methods for complex fin analysis.

One of the key parameters that can enhance the heat transmission rate is the thermal conductivity of the nanoparticles. Thermal conductivity refers to the ability of the nanoparticles to conduct heat. Due to its surface scattering processes and size effects, it differs from the bulk material.

They are chosen in heat transmission applications to increase the heat transfer rate, since they have better thermal conductivity compared to their bulk counterparts. The factors effecting the stability, thermal conductivity of nanofluid and its applications were analysed and evaluated [15-18]. Apart from thermal conductivity, the shape of nanoparticles influences the heat flow. This idea has been explored by researchers in their analysis to study its effect on the rate of heat transfer. The effect of shape factor of nanoparticles on the flow characteristics of hybrid nanofluids and the thermal efficiency of fins wetted with hybrid nanofluids were investigated and analysed [19-22]. The result indicates a substantial improvement in thermal efficiency. The thermal behaviour of moving longitudinal fin in shape dependent $H_2O–C_2H_6O_2$/GO–MoS_2 hybrid nanofluid was analysed by Talbi *et al.,* [23]. The numerical solution for the governing equation was obtained using RKFT45 and analytically with Duan – Rach approach. AlBaidani *et al.,* [24] came up with an idea to make the fin more effective and proposed annular fin in ternary hybrid nanofluid. Analysis was carried out for various shapes of nanoparticles. In addition, volume fraction i.e the ratio of volume nanoparticles to the overall volume of nanofluid impacts the rate of heat flow. It effects the thermal conductivity, in turn influencing the rate of heat transfer [25-28]. The addition of spinning nanoparticles to the base fluid can enhance the heat transmission rate. Al-Hossainy and Eid [29] explored this idea. Experimental and computational studies conducted by them on the PEG-H_2O/ZrO_2+MgO combination showed an increase in the rate of heat transfer. Venkatesan *et al.,* [30] analyzed the flow of heat in automotive radiator using Al_2O_3 – SiC in ethylene glycol base fluid. The analysis was carried using ANSYS FLUENT Software and found 12% - 15% increase in radiator efficiency. Akbar *et al.,* [31] analyzed the thermal profile of stretching sheet under the influence of base fluid with copper nanoparticles of various shapes. Alkasasbeh [32] carried out the analysis of vertical stretching sheet wetted with Casson hybrid nanofluid in the presence of magnetic field. ODEs were solved using CDQ method and the effect of Casson parameter, magentic field were studied. The result indicates an increase in the thermal profile and decrease in the velocity profile with the increase in Casson parameter and magnetic field. Increasing the porosity parameter decreases the skin friction coefficient and heat transfer rate, as demonstrated by Saupi *et al.,* [33] on a permeable stretching sheet embedded in a porous medium using a magnetohydrodynamic hybrid copper-alumina nanofluid. Muhammad and Che Sidik [34] analyzed the influence of various microchannel configurations with nanofluid on the heat transfer performance of cooling systems. The heat transfer enhances with the increase in the particles Reynolds number and concentration. Elfaghi *et al.,* [35] investigated the heat transfer performance of circular pipe with Al_2O_3/H_2O nanofluid by analysing the effects of concentration and reynolds number. Sidik and Alawi [36] carried out the numerical simulation of heat transfer in a concentric annulus embedded with different nanorefrigerants. It was observed that the SiO_2 nanoparticle had the highest Nusselt number followed by Al_2O_3, ZnO, CuO and lowest value for pure refrigerant.

Despite the rapid advancements in nanofluid based cooling systems, there are still gaps in understanding the impact of various similarity parameters on the overall thermal performance of these systems. While the previous studies have investigated the various types of nanofluid, the combination of Al_2O_3 and SiC nanoparticles in hybrid nanofluid integrated with a heat sink have not been extensively studied. In addition, the studies have focused on idealized boundary conditions, overlooking the practical implications of convective and insulated boundary conditions. The proposed model addresses these gaps by providing insights into the concentration, boundary conditions and the shape of the nanoparticles on the thermal performance of the system, as well as the effectiveness of these hybrid nanofluids in improving the heat transfer rate in practical engineering applications. Heat transfer analysis researchers continue to focus on the increasing requirement for efficient thermal management, which is a result of the rising heat density in compact

heat exchangers across a variety of small devices and technological processes. The objective of this investigation is to optimize the heat transfer performance of the proposed Integrated Hybrid Nanofluid Heat Sink Model by examining the combined effects of novel combination of Al₂O₃ – SiC nanoparticles on the thermal characteristics of the fin. Both Al₂O₃ and SiC nanoparticles possess excellent thermal conductivity, allowing efficient heat dissipation. Their hardness, stability and resistance to corrosion allows their usage in the harsh environment. Silicon carbide can be used in high power electronic devices due its wide bandgap and its light weight makes it useful in aerospace and automotive industries. The novelty of this work lies in the effective utilization of novel combination of nanoparticles of various shapes and analyzing its effect on the thermal performance of the fin by obtaining the solution to the governing equations using *three stage Lobatto quadrature* numerical technique with suitable boundary conditions. The investigation of our proposed model shows a considerable improvement in the heat transfer rate. A comparative analysis was performed between the convective and insulated fin tips. Furthermore, the effect of changing the shapes of nanoparticle on the heat transfer rate was analyzed. The formulated equations were numerically solved, and the results were comprehensively discussed through graphical interpretation.

2. Methodology

In our proposed *"Integrated hybrid nanofluid heat sink model (IHNFHSM)"*, we have considered a moving penetrable longitudinal moving fin with uniform cross- sectional area wetted with Al₂O₃–SiC/H₂O hybrid nanofluid of different nanoparticle shapes. The arrangement is depicted in Figure 1. Darcy's model was employed in the analysis due to the fin porosity. It is assumed that the fin is initially at rest position with the base temperature T_b' and ambient temperature T_a'. Subsequently, the horizontal movement of the fin with a steady velocity U' results in a loss of heat due to radiation and natural convection. In addition, to enable the simplification of partial differential equation to ordinary differential equation, the temperature and flow characteristics is assumed to exhibit no variation with respect to time. A well-defined boundary condition is established by assuming the temperature of the surrounding medium of the fin to be constant. To simplify the model, few parameters such as thermal conductance at the interface, contact area, contact pressure and surface roughness are eliminated by assuming the contact resistance between the fin base and the prime surface to be negligible. The fin's base temperature is assumed constant to enhance the computational efficiency and the accuracy of the numerical simulation, as it facilitates a well-defined boundary condition that serves as a reference point for the temperature distribution along the fin. To reduce the variation in nanoparticle properties and maintain consistent thermal properties and heat transfer, Al₂O₃ – SiC nanomaterials and liquid in the continuous phase are assumed to be in the thermal equilibrium state.

The governing thermal equilibrium equation of a fin at cross-section $'dx''$ in hybrid nanofluid is given by

$$\frac{d^2T'}{dx'^2} - \frac{(\rho c_p)_{hnf} U'}{k'_{hnf}} \frac{dT'}{dx'} - \frac{2h_D i_{fg}(1-\overline{\phi})(\omega'-\omega_a')}{tk'_{hnf}} - \frac{2\varepsilon\sigma F_{f-a}(T'^4)}{tk'_{hnf}} - \frac{2\varepsilon\sigma F_{f-a}(T_a'^4)}{tk'_{hnf}} - \frac{2h'(1-\overline{\phi})(T'-T_a')}{tk'_{hnf}} -$$

$$\frac{2g(\rho)_{hnf}(c_p)_{hnf}K(\rho)_{hnf}(\beta)_{hnf}\left(T'^2+T_a^2-2T_aT'\right)}{k'_{hnf}\mu_{hnf}t} = 0 \tag{1}$$

where β_{hnf} is the volumetric coefficient of thermal expansion, μ_{hnf} the effective dynamic viscosity, $(C_p)_{hnf}$ specific heat with constant pressure, k'_{hnf} thermal conductivity, ρ_{hnf} effective density, U' Constant velocity of the fin and T' local temperature of the fin. The subscript nf and hnf for nanofluid and hybrid nanofluid. x' denotes axial distance, h_D represents uniform mass transfer

Coefficient, ε Surface emissivity of fin, σ Stefan Boltzmann constant, ω' Saturated air humidity ratio, ω'_a Surrounding air humidity ratio, K Permeability, g Acceleration due to gravity, F_{f-a} the shape factor for radiation heat transfer, h' Heat transfer coefficient, $\overline{\overline{\emptyset}}$ Porosity, i_{fg} Latent heat of water evaporation and t fin thickness.
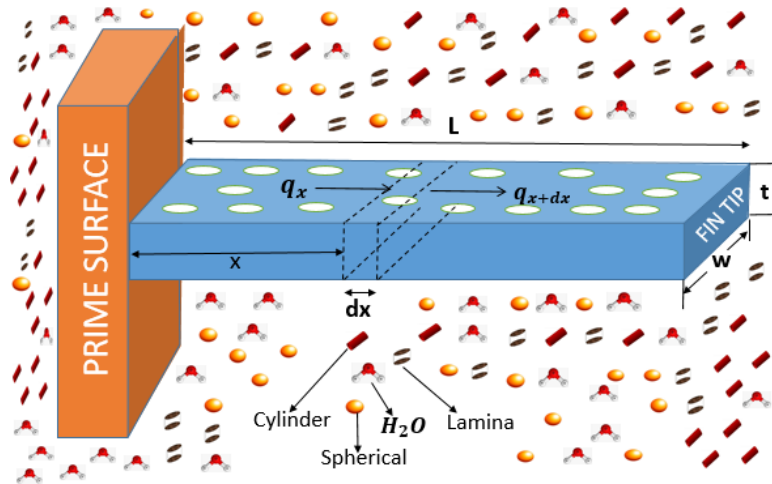
Fig. 1. Schematic of proposed *IHNFHSM*

Mathematically, it is addressed as

$$k'_{hnf} = \frac{k'_{nf}\left(k'_{p_2}+(\alpha'-1)k'_{nf}\right)-(\alpha'-1)\emptyset_2\left(k'_{nf}-k'_{p_2}\right)}{\left(k'_{p_2}+(\alpha'-1)k'_{nf}\right)+\emptyset_2\left(k'_{nf}-k'_{p_2}\right)} \tag{2}$$

$$k'_{nf} = \frac{k'_f\left(k'_{p_1}+(\alpha'-1)k'_f\right)-(\alpha'-1)\,\emptyset_1 k'_f(k'_f-k'_{p_1})}{\left(k'_{p_1}+(\alpha'-1)k'_f\right)+\emptyset_1(k'_f-k'_{p_1})} \tag{3}$$

where α' is the shape factor of nanoparticles. For a spherical shape, $\alpha' = 3$.

$$\mu_{hnf} = \frac{\mu_f}{[(1-\emptyset_2)(1-\emptyset_1)]^{2.5}} \tag{4}$$

$$\rho_{hnf} = \left[(1-\emptyset_1)(1-\emptyset_2)\rho_f + \emptyset_1\rho_{p_1}(1-\emptyset_2)\right] + \emptyset_2\rho_{p_2} \tag{5}$$

$$(\rho c_p)_{thnf} = \left[(1-\emptyset_1)(1-\emptyset_2)(\rho c_p)_f + \emptyset_1(1-\emptyset_2)(\rho c_p)_{p_1}\right] + \emptyset_2(\rho c_p)_{p_2} \tag{6}$$

$$(\rho\beta)_{thnf} = \left[(1-\emptyset_2)(1-\emptyset_1)(\rho\beta)_f + \emptyset_1(1-\emptyset_2)(\rho\beta)_{p_1}\right] + \emptyset_2(\rho\beta)_{p_2} \tag{7}$$

Subscript p_1 and p_2 stand for solid nanoparticles (Al₂O₃) and (SiC) respectively, whereas $\emptyset_1\ and\ \emptyset_2$ represents the solid volume fraction of Al₂O₃ and SiC.

The thermal properties of Al₂O₃ ₋ SiC/ H₂O nanofluid along with their physical properties are listed in Table 1. The coefficient of heat transfer h' is defined as

$$h' = \left[\frac{(T'_a-T')^n}{(T'_a-T'_b)^n}\right]h'_a \tag{8}$$

where h_a' is the convective heat transport coefficient at temperature T_a' .

Table 1
Properties of each content of hybrid nanofluid

Physical Properties	ρ (Kgm^{-3})	c_p $(JKg^{-1}K^{-1})$	k' $(Wm^{-1}K^{-1})$	β (K^{-1})
Al₂O₃	3970	765	40	0.87×10^{-5}
SiC	3210	750	120	0.277×10^{-5}
Water	997.2	4179	0.614	2.1×10^{-4}

Two types of boundary condition are used to solve the differential equation Eq. (1)

Case I: Insulated fin tip.

$$T'(0) = T_b' \quad at \; x' = 0$$
$$\frac{dT'(L)}{dx'} = 0 \quad at \; x' = L \tag{9}$$

Case II: Convective fin tip.

$$T'(0) = T_b' \quad\quad\quad at \; x' = 0$$
$$h_a'T'(L) + k_{hnf}' \frac{dT'(L)}{dx'} = 0 \quad at \; x' = L \tag{10}$$

where L is the fin length.

The following parameters are used to non-dimensionalize the differential equation Eq. (1)

$$\omega' - \omega_a' = b_2 T' - T_a' b_2, \; \theta = \frac{T'}{T_b'}, \; \theta_a = \frac{T_a'}{T_b'}, \; X = \frac{x'}{L}, \; Nc = \frac{2(\rho C_p)_f (\rho\beta)_f gKT_b'L^2}{k_f'\mu_f t}, \; Nr = \frac{2\varepsilon\sigma L^2 T_b'^3}{t\,k_f'}, \; Pe =$$
$$\frac{(\rho C_p)_f U'L}{k_f'}, \; Bi = \frac{h_a'L}{k_f'}, \; m_1 = \frac{2b_2 L^2 h_a' i_{fg}(1-\bar\phi)}{(Le)^{2/3} tC_{pf}k_f'}, \; m_0 = \frac{2L^2 h_a'(1-\bar\phi)}{tk_f'}, \; m_1 = m_2 - m_0 \tag{11}$$

The ODE in dimensionless form is obtained by substituting Eq. (8) and Eq. (11) in Eq. (1)

$$\frac{d^2\theta}{dX^2} - pe\left(\frac{(\rho C_p)_{hnf}}{(\rho C_p)_f}\right)\left(\frac{k_f'}{k_{hnf}'}\right)\left(\frac{d\theta}{dX}\right) - Nr\left(\frac{k_f'}{k_{hnf}'}\right)(\theta^4 - \theta_a^4)$$
$$-(m_1 + m_0)\frac{(\theta-\theta_a)^{1+n}}{(1-\theta_a)^n}\left(\frac{k_f'}{k_{hnf}'}\right) - Nc(\theta - \theta_a)^2 \left(\frac{\mu_f}{\mu_{hnf}}\right)\left(\frac{k_f'}{k_{hnf}'}\right)\left(\frac{(\rho\beta)_{hnf}}{(\rho\beta)_f}\right) = 0 \tag{12}$$

The non-dimensionalized boundary conditions:

$$\begin{cases} \theta(X) = 1 & at \; X = 0 \\ \theta(X) = 0 & at \; X = 1 \end{cases} \text{insulated tip and}$$
$$\begin{cases} \theta(X) = 1 & at \; X = 0 \\ \left(\frac{d\theta}{dX}\right) = -\theta(X)\frac{k_f'}{k_{hnf}'} Bi & at \; X = 1 \end{cases} \text{convective tip} \tag{13}$$

where $Nc, Nr, \Theta_a, Bi, m_2$, n and Pe are convective parameter, radiative parameter, non-dimensional ambient temperature, Biot number, wet porous parameter, power index, and peclet number respectively. The dimensionless temperature and the axial distance are θ and, where as m_1 and m_0 are constants.

2.1 Numerical Solution

The nonlinear differential equation in Eq. (12) is solved using the *three stage Lobatto quadrature* numerical technique, as it offers excellent stability and convergence for solving boundary value issues. The dimensionless governing equation is rewritten as

$$\theta''(X) = -(m_1 + m_0)\frac{(\theta-\theta_a)^{1+n}}{(1-\theta_a)^n}\left(\frac{k'_f}{k'_{hnf}}\right) pe\left(\frac{(\rho C_p)_{hnf}}{(\rho C_p)_f}\right)\left(\frac{k'_f}{k'_{hnf}}\right)\theta'(X) - Nr\left(\frac{k'_f}{k'_{hnf}}\right)(\theta^4 - \theta_a^4) -$$

$$Nc(\theta - \theta_a)^2 \left(\frac{\mu_f}{\mu_{hnf}}\right)\left(\frac{k'_f}{k'_{hnf}}\right)\left(\frac{(\rho\beta)_{hnf}}{(\rho\beta)_f}\right) \tag{14}$$

Where $\theta''(X) = \frac{d^2(\theta)}{dx^2}$ and $\theta'(X) = \frac{d\theta}{dx}$.

Integrating $\theta''(X)$ from X_0 to $X_1 = X_0 + h$, where h is the interval length, the system of integral equations are given by

$$\theta(X_1) = \theta(X_0) + h\,\theta'(X_0) + h^2 \int_{X_0}^{X_1}(1-t)\theta''(X_0 + ht)\,dt \tag{15}$$

$$\theta'(X_1) = \theta'(X_0) + \int_{X_0}^{X_1}\theta''(t)\,dt \tag{16}$$

Applying four-point quadrature formula to solve the integral Eq. (15) and Eq. (16) to move from

X_i to $X_{i+1} = X_i + h, i = 0, 1, 2, 3, \ldots\ldots\ldots\ldots\ldots\ldots$

$$\theta_{i+1.3819} = \theta_i + 1.3819h\theta'_i + 0.9549h^2\theta''_i \tag{17}$$

$$\theta_{i+3.6180} = \theta_i + 3.6180h\theta'_i + 6.5450h^2\theta''_i \tag{18}$$

$$\theta'_{i+1.3819} = \frac{-16.4852}{h}\theta_i - 1.4721\theta'_i - 0.0427h\theta''_i + \frac{17.2360}{h}\theta_{i+1.3819} + \frac{0.2492}{h}\theta_{i+3.6180} \tag{19}$$

$$\theta'_{i+3.6180} = \frac{67.4852}{h}\theta_i + 5.2360\theta'_i + 0.2927h\theta''_i + \frac{12.7639}{h}\theta_{i+3.6180} - \frac{80.2492}{h}\theta_{i+1.3819} \tag{20}$$

$$\theta_{i+2.7639} = \theta_i + 2.7639h\theta'_i + 1.2732h^2[\theta''_i + 2\,\theta''_{i+1.3819}] \tag{21}$$

$$\theta_{i+7.2360} = \theta_i + 7.2360h\theta'_i + 8.7267h^2[\theta''_i + 2\,\theta''_{i+3.6180}] \tag{22}$$

$$\theta'_{i+2.7639} = \frac{-8.7426}{h}\theta_i - 1.4721\theta'_i - 0.0854h\theta''_i + \frac{6.3819}{h}\theta_{i+2.7639} + \frac{0.1246}{h}\theta_{i+7.2360} \tag{23}$$

$$\theta'_{i+7.2360} = \frac{33.7426}{h}\theta_i + 7.4721\theta'_i + 0.5854h\theta''_i + \frac{8.6180}{h}\theta_{i+7.2360} - \frac{40.1246}{h}\theta_{i+2.7639} \tag{24}$$

$$\theta_{i+1} = \theta_i + h\theta'_i + \frac{h^2}{12}[\theta''_i + 5(7.2360\,\theta''_{i+2.7639} + 2.7639\,\theta''_{i+7.2360})] \tag{25}$$

$$\theta'_{i+1} = \theta'_i + \frac{h}{12}[\theta''_i + 5(\theta''_{i+r} + \theta''_{i+s}) + \theta''_{i+1}] \tag{26}$$

where $\theta_i = \theta(X_i)$, $\theta'_i = \theta'(X_i)$, $\theta''_i = \theta''(X_i)$, $\theta_{i+1.3819} = \theta(X_i + 1.3819h)$, $\theta_{i+3.6180} = \theta(X_i + 3.6180h)$, $\theta_{i+2.7639} = \theta(X_i + 2.7639h)$, $\theta_{i+7.2360} = \theta(X_i + 7.2360h)$, $\theta'_{i+2.7639} = \theta'(X_i + 2.7639h)$, $\theta'_{i+7.2360} = \theta'(X_i + 7.2360h)$, $\theta''_{i+2.7639} = \theta''(X_i + 2.7639h)$, $\theta''_{i+7.2360} = \theta''(X_i + 7.2360h)$ $\theta_{i+1} = \theta(X_i + h)$, $\theta'_{i+1} = \theta'(X_i + h)$

Eq. (17) to Eq. (26) are solved for convective and insulated tip boundary conditions to obtain the fin dimensionless temperature $\theta(X_i)$ and temperature gradient $\theta'(X_i)$ using MATLAB simulation tool.

3. Results

The validation of the *Lobatto* numerical technique is given in Table 2. It displays the comparison of the numerical values of $\theta(X)$ using *Lobatto* numerical technique with the existing values [20]. It is evident that the obtained values closely match the expected values. Furthermore, Table 3 shows the Convective fin tip temperature $\theta(X)$ in *Nanofluid* and *Hybrid Nanofluid* mixtures at $X = 1$ for $\emptyset_1 = 0.04, \emptyset_2 = 0.04$ and various values of similarity parameter, as well as the percentage change in the temperature by changing the nanoparticle mixture in base fluid from Al_2O_3 to $Al_2O_3 - SiC$.

Table 2
Validation of the *Lobatto* numerical technique at $X = 1$ with the existing result of Gireesha *et al.,* [20] for $\emptyset_1 = 0.04, \emptyset_2 = 0.04, Nc = 10, Nr = 5, n = m_2 = 1, Pe = 2, \theta_a = 0.2$

| X	$\theta(X)$ RKF Numerical Technique [20]	$\theta(X)$ Lobatto Numerical Technique	Absolute Error
0	1.000000000000	1.000000000000	0.000×10^{-9}
0.2	0.743440385716	0.743440385414	0.301×10^{-9}
0.4	0.598468327898	0.598468327788	0.110×10^{-9}
0.6	0.503973665640	0.503973665541	0.099×10^{-9}
0.8	0.432174231270	0.432174231203	0.067×10^{-9}
1	0.371433068027	0.371433068015	0.012×10^{-9}

Table 3
Convective fin tip temperature $\theta(X)$ in *Nanofluid* and *Hybrid Nanofluid* at $X = 1$ for $\emptyset_1 = 0.04, \emptyset_2 = 0.04$ and various values of similarity parameter

Pe	θ_a	n	Bi	m_2	Nr	Nc	*Nanofluid* Al_2O_3 / H_2O $\theta(X)$	*Hybrid Nanofluid* $Al_2O_3 - SiC/ H_2O$ $\theta(X)$	*% Change in fin temperature* $\theta(X)$
0.5	0.2	1	1	1	2	1	0.464880	0.481463	3.567157
						10	0.384554	0.404975	5.310308
						50	0.272198	0.289597	6.392038
					1	10	0.371929	0.400741	7.746640
					5		0.348073	0.372374	6.981581
					10		0.326894	0.347836	6.406358
				0.1			0.354511	0.379654	7.092305
				1			0.346831	0.370895	6.938249
				10			0.296087	0.313621	5.921908
			1				0.346831	0.370895	6.938249
			2				0.276808	0.298879	7.973397
			3				0.228632	0.248549	8.711379

3.1 Effect of Peclet Number

Figure 2(a) and Figure 2(b) show how the Peclet number (Pe) effects the heat flow in a fin with convective and insulated tips. As a general trend, an increment in the Peclet number leads to rise in the fin temperature profile. This is attributed to the accelerated movement of the fin with higher Pe values, which consequently reduces the exposure time of the fin to the environment, resulting in an overall enhancement in temperature. For a convective tip, increasing the Pe value by 100% resulted in an 8.77% increase in the temperature distribution profile.
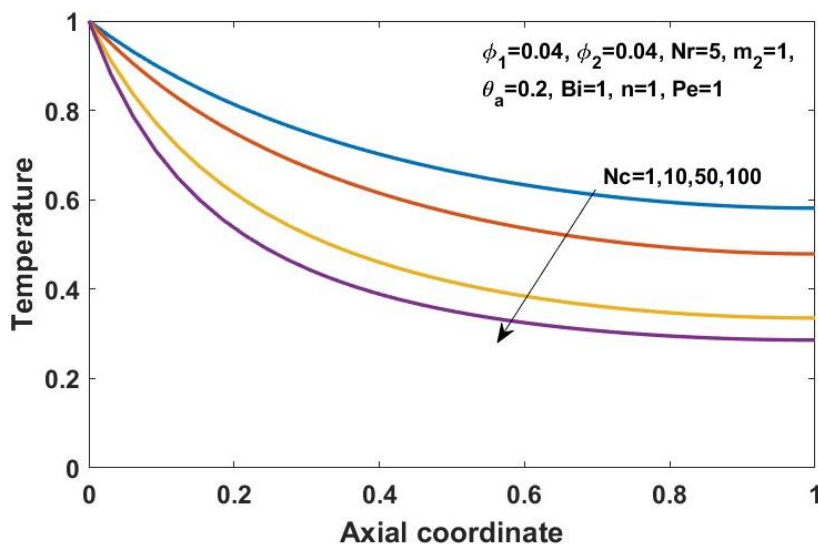

(a)
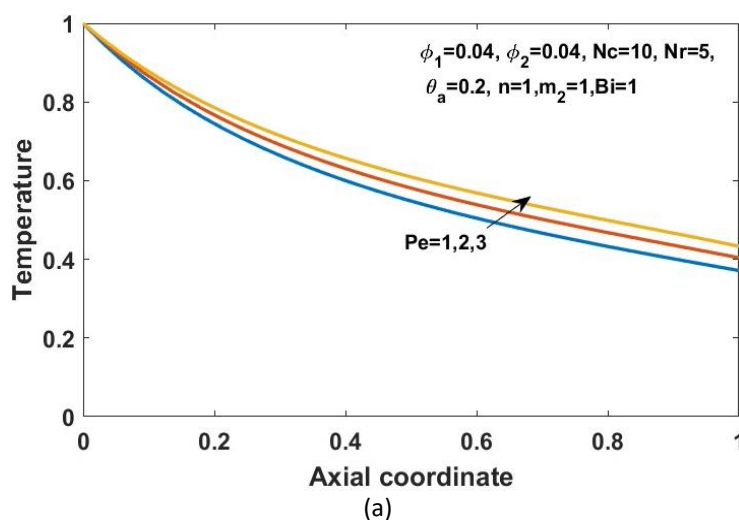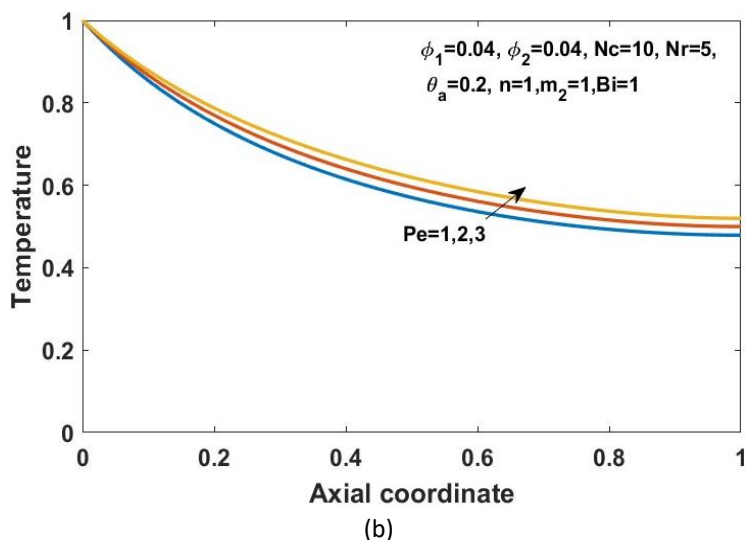
Fig. 2. Repercussion of Peclet numbers 1, 2, and 3 on dimensionless temperature of a fin (a) with convective tip and (b) with insulated tip

3.2 Effect of Convective Parameter

The convective heat transfer performance of hybrid nanofluids is quantitatively characterized using convective parameter (Nc). The dimensionless fin temperature for different values of Nc is depicted in Figure 3(a) and Figure 3(b). It is visible that the temperature distribution towards the tip of the fin reduces with the rise in the Nc values, which means temperature is uniformly distributed along the fin. If we relate this to Darcy's model, as convective parameter increases the Darcy's number increases, thereby influencing the rise in Buoyancy or permeability effect, which will ease the fluid flow in porous medium. From the simulation result obtained, an increment in the Nc value by 100%, the dimensionless fin temperature for a convective tip reduces by 13.68% implying a rapid flow of fluid through the pores, thereby enhancing the heat transfer rate of the proposed *IHNFHSM*.
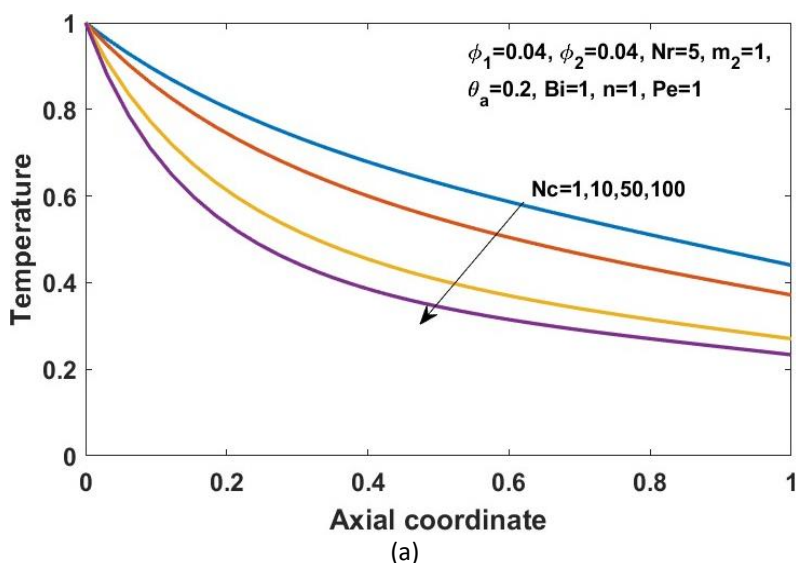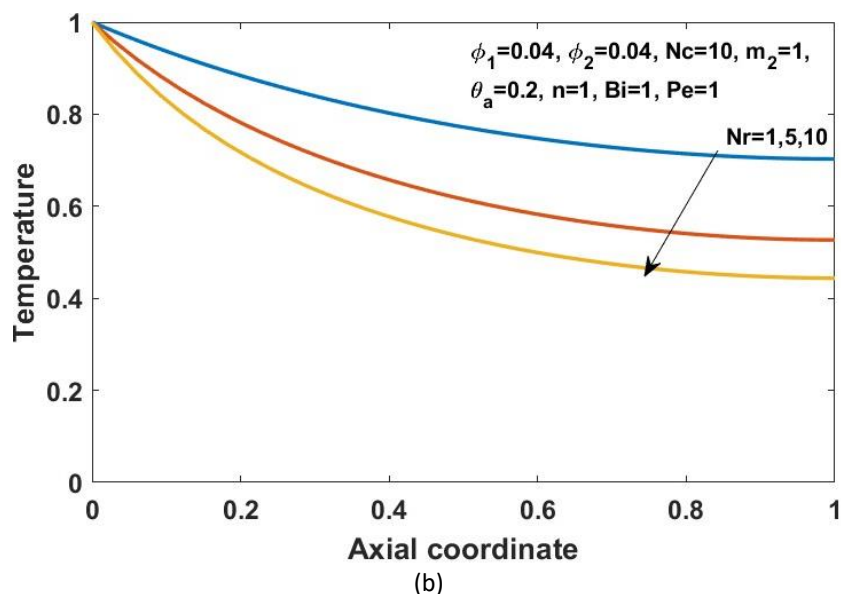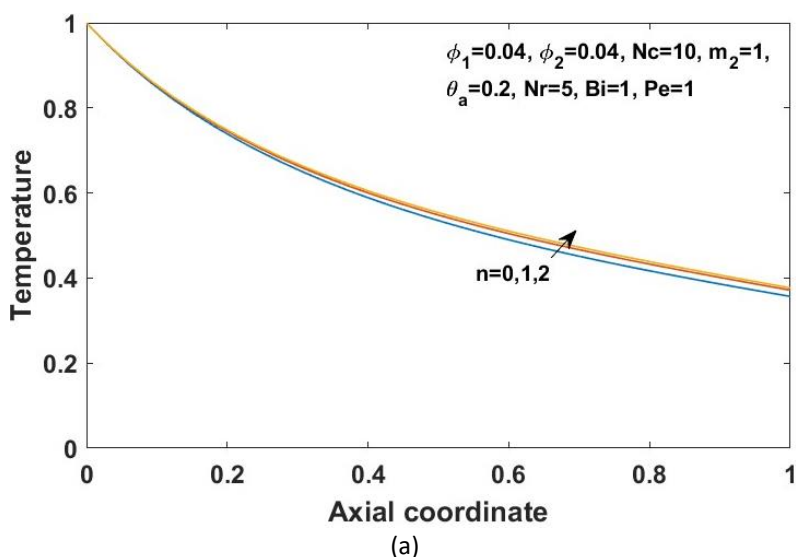
Fig. 3. Repercussion of Nc on dimensionless temperature of a fin (a) with convective tip and (b) with insulated tip

3.3 Effect of Radiative Parameter

The influence of the radiative parameter Nr on the temperature distribution is shown below in Figure 4(a) and Figure 4(b). Increasing the value of radiative parameter decreases the temperature profile along the fin length. This implies that the radiation effect from the fin gets stronger as we increase the radiation parameter, and more heat is radiated away from fin surface to the surrounding hybrid nanofluid. From the simulation, it was observed that an increment in Nr value by 100%, the temperature distribution towards the tip of the fin is reduced by 6.46%, implying that the system is cooling the fin at a faster rate leading, thereby enhancing the heat transfer rate of the proposed *IHNFHSM*.
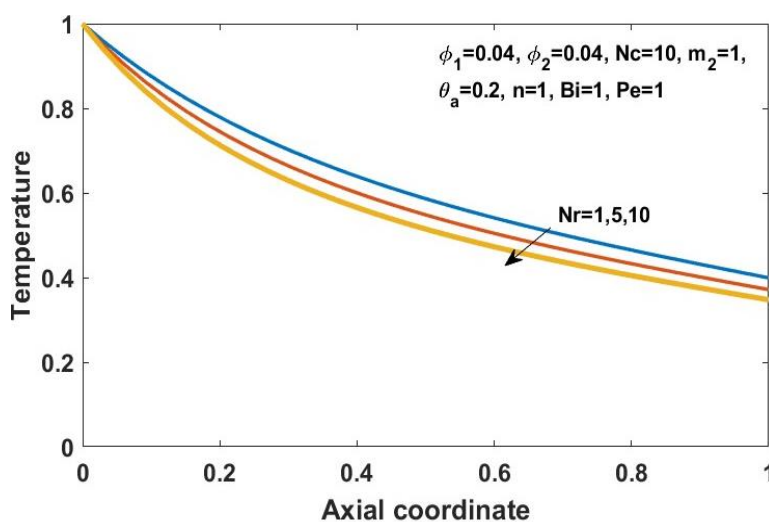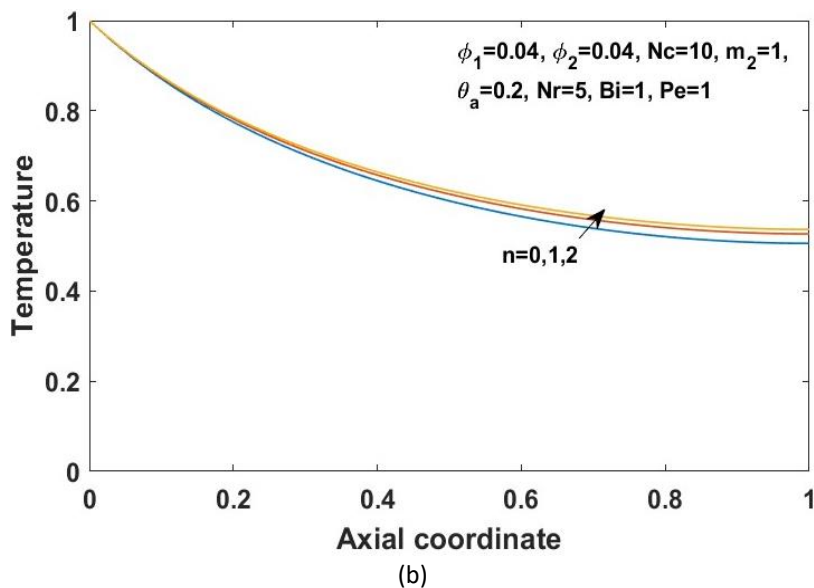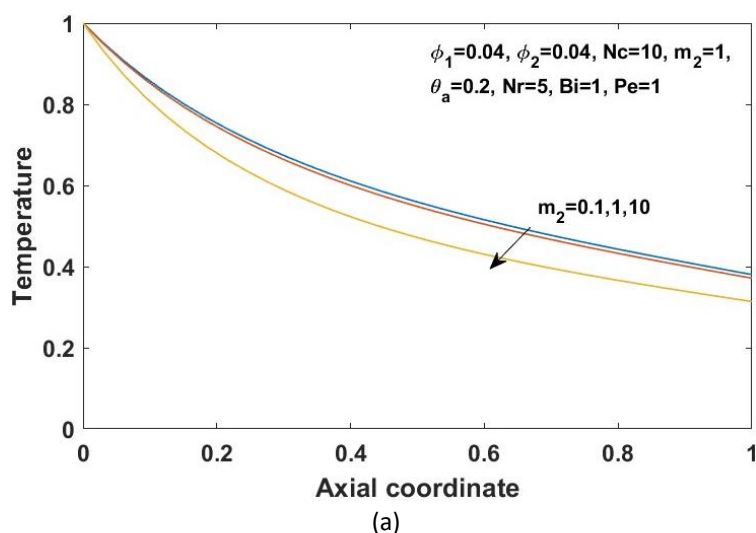
Fig. 4. Repercussion of Nr on dimensionless temperature of a fin (a) with convective tip and (b) with insulated tip

3.4 Effect of Power Index

Figure 5(a) and Figure 5(b) display the effect of power index 'n' on the dimensionless fin temperature for convective and insulated tip. Power index 'n' represents the flow regime of the hybrid nanofluid. Increase in the value of 'n' parameter, increases the dimensionless fin temperature, as the fluid gains more resistance due to increase in non-linearity in its flow. For smaller values of 'n' value, fluid flow is linear and the heat is efficiently dissipated from the fin due to lower resistance, keeping the fin cooler. In this case, the temperature gradient between the fin and the fluid is higher, thereby increasing the overall heat transfer rate of the system. From our simulations, it was observed that increasing the value of 'n' by 100%, the temperature profile rises by 1.4%.
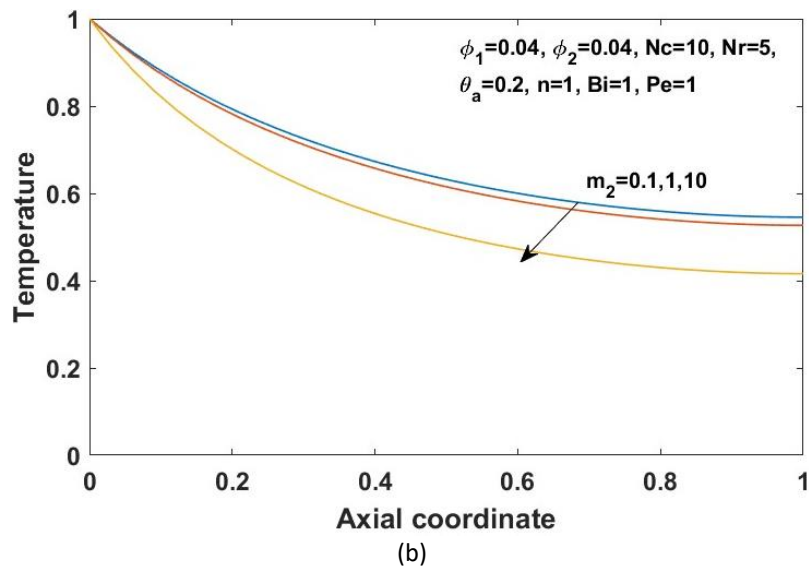
Fig. 5. Repercussion of n on dimensionless temperature of a fin (a)
with convective tip and (b) with insulated tip

3.5 Effect of Wet Porous Parameter

Figure 6(a) and Figure 6(b) display the influence of wet porous (m_2) parameter on the dimensionless fin temperature for convective and insulated tips. It is evident from the variation that the increase in the m_2 value reduces the fin temperature, indicating a rapid flow of fluid through the porous medium compared to the free flow, which in turn enhances the convection at the surface of the fin. The simulation results obtained for the proposed model shows that the temperature distribution at the convective tip of the fin improves by approximately 9%. This implies that the increase in m_2 value leads to higher surface area for heat transfer, leading to an enhancement in the heat transfer rate.
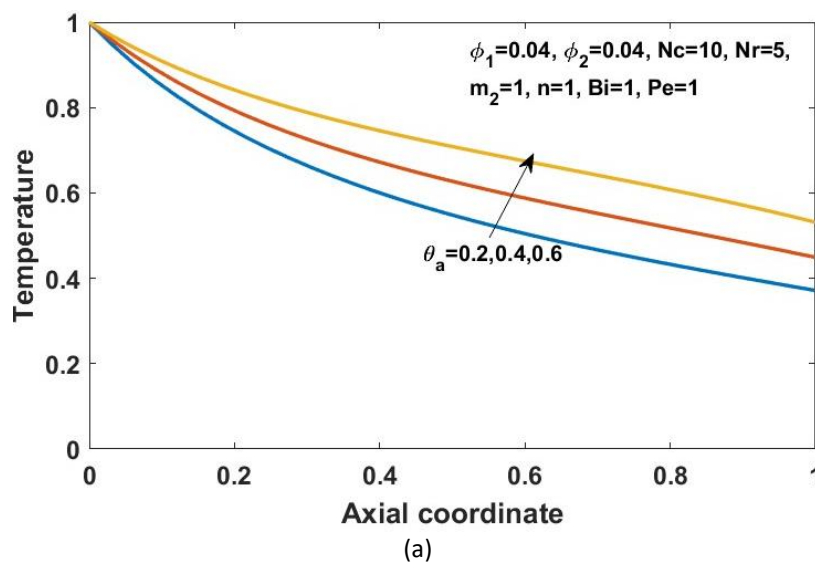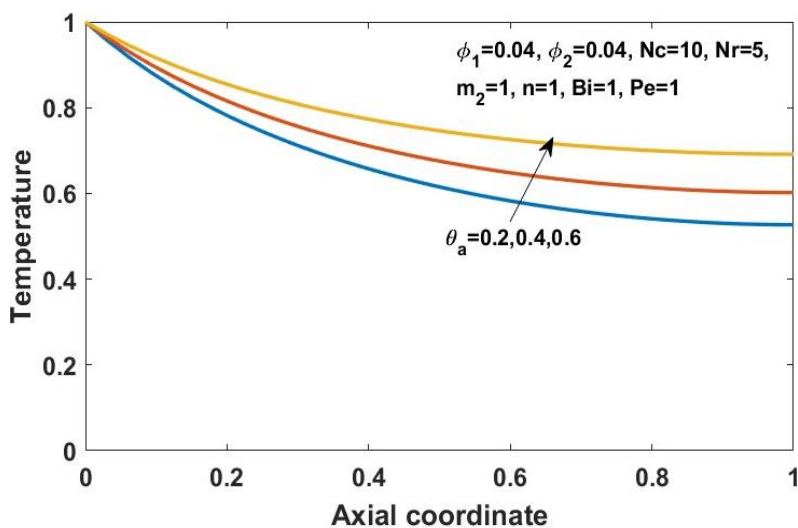
Fig. 6. Repercussion of m₂ on dimensionless temperature of a fin (a) with convective tip and (b) with insulated tip

3.6 Effect of Ambient Temperature

The impact of ambient temperature on the temperature gradient along the fin's surface is depicted in Figure 7(a) and Figure 7(b). An enhancement of θ_a enhances the surrounding liquid temperature, in turn reducing the change in the temperature between the fin and the surrounding. This hampers the heat transfer from the surface of the fin, leading to rise in the fin temperature. The simulation results obtained shows that a rise of 100% in the ambient temperature θ_a, enhances the temperature profile by 15.5% at the convective tip of the fin.

(b)

Fig. 7. Repercussion of ambient temperature on dimensionless temperature of a fin (a) with convective tip and (b) with insulated tip

3.7 Effect of Biot Number

Biot number 'Bi' plays a crucial role in understanding the thermal performance of the system. Its impact is graphically illustrated in Figure 8. As the value of Bi increases, the convective heat transfer becomes more predominant than conductive heat transfer, causing a larger temperature gradient between the fin and the nanofluid. This results in an increased heat flow rate from the fin to the nanofluid, eventually reducing the temperature of the fin at a faster rate. The simulation result obtained of the proposed model shows that the dimensionless temperature at the tip of the fin decreases by 19.41% with 100% increase in Biot number, thereby enhancing the thermal performance of the system.
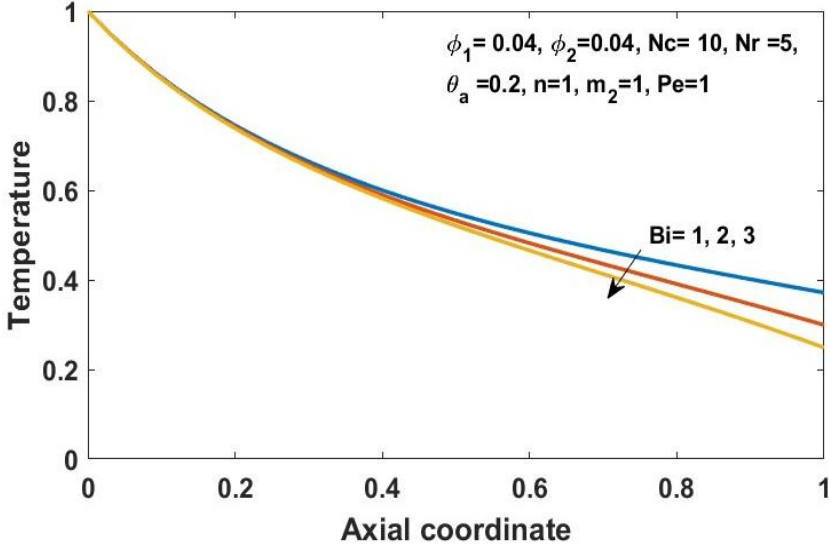

Fig. 8. Dimensionless fin temperature of convective tip for various Bi values

3.8 Optimization of Parameters

The overall thermal performance of the *IHNFHSM* is depicted in the Figure 9 to Figure 12 in the form of variation in the heat transfer rate $-\theta'(0)$ with respect to Nc, Nr and m$_2$ values, for both convective and insulated tips. The variation clearly shows an enhancement in the rate of heat transfer with an increment in the values of Nc, Nr and m$_2$. In case of convective fin tip, an enhancement in the heat transfer rate was observed compared to an insulated fin tip. Quantitatively, at Nc= Nr = m$_2$ =1, the heat transfer rate of convective fin tip was enhanced by 2.94%, 32.88% and 16.3% compared to an insulated fin tip. Figure 12 depicts the percentage enhancement in heat transfer rate with 100% rise in Nc, Nr and m$_2$ values. It is observed that the maximum enhancement in the rate of heat transfer occurs when the value of Nc changes two-fold from 20 to 40, Nr *changes* from 10 to 20 and m$_2$ from 5 to 10. For optimized heat transfer rate, Nc, Nr and m$_2$ values can be adjusted in the range of 10 to 20.
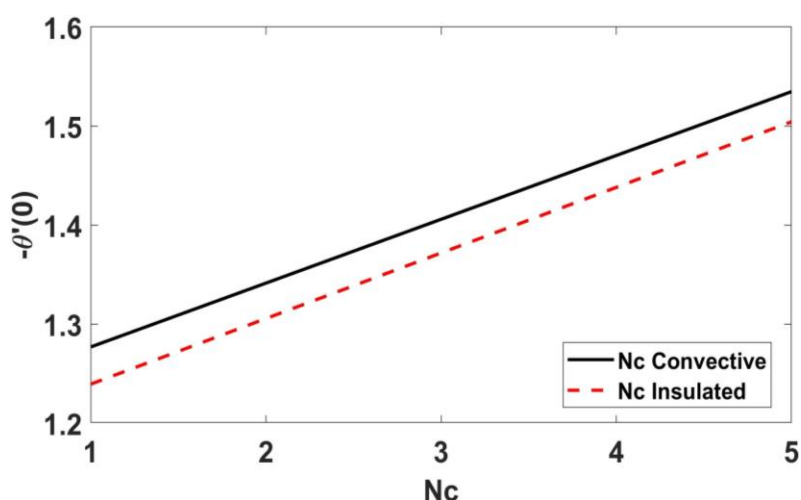

Fig. 9. Heat transfer rate of *IHNFHSM* for various values of Nc for $\emptyset_1 = 0.04, \emptyset_2 = 0.04$, Pe=2, Nr=5, n=1, m$_2$ = 1, θ_a= 0.2, Bi=1
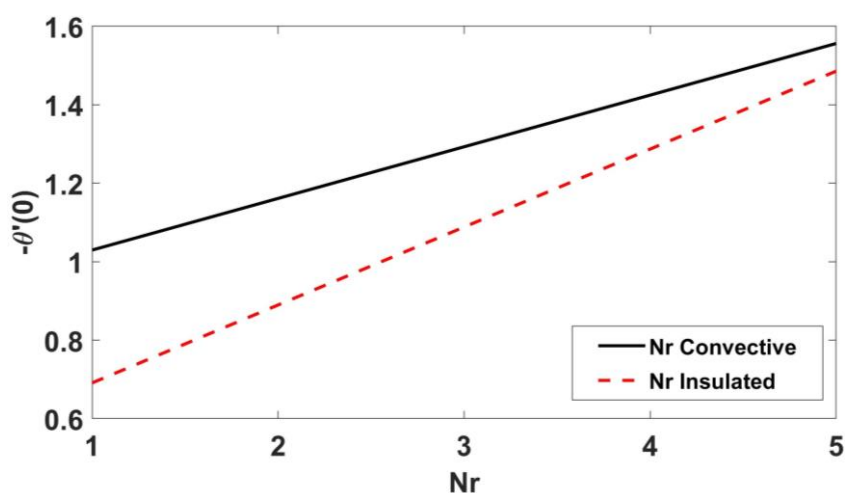

Fig. 10. Heat transfer rate of *IHNFHSM* for various values of Nr for $\emptyset_1 = 0.04, \emptyset_2 = 0.04$, Pe=2, Nc=10, n=1, m$_2$ = 1, θ_a= 0.2, Bi=1
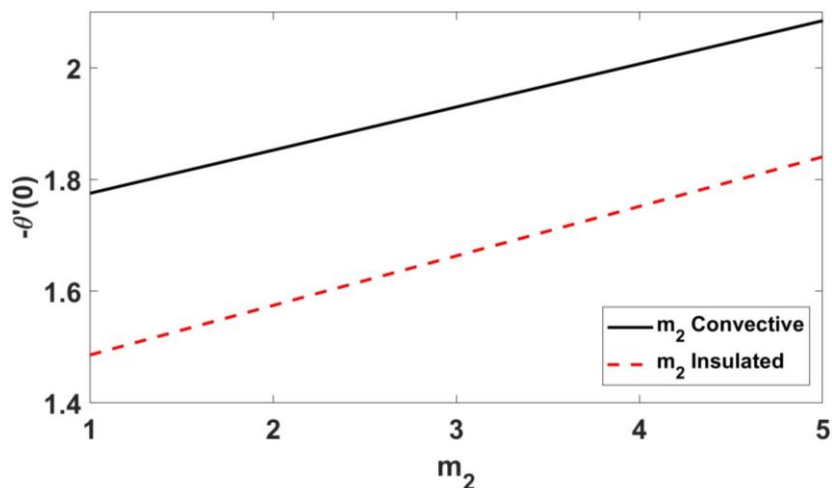
Fig. 11. Heat transfer rate of *IHNFHSM* for various values of m_2 for $\emptyset_1 = 0.04, \emptyset_2 = 0.04$, Pe=2, Nc=10, Nr=5, n=1, θ_a= 0.2, Bi=1

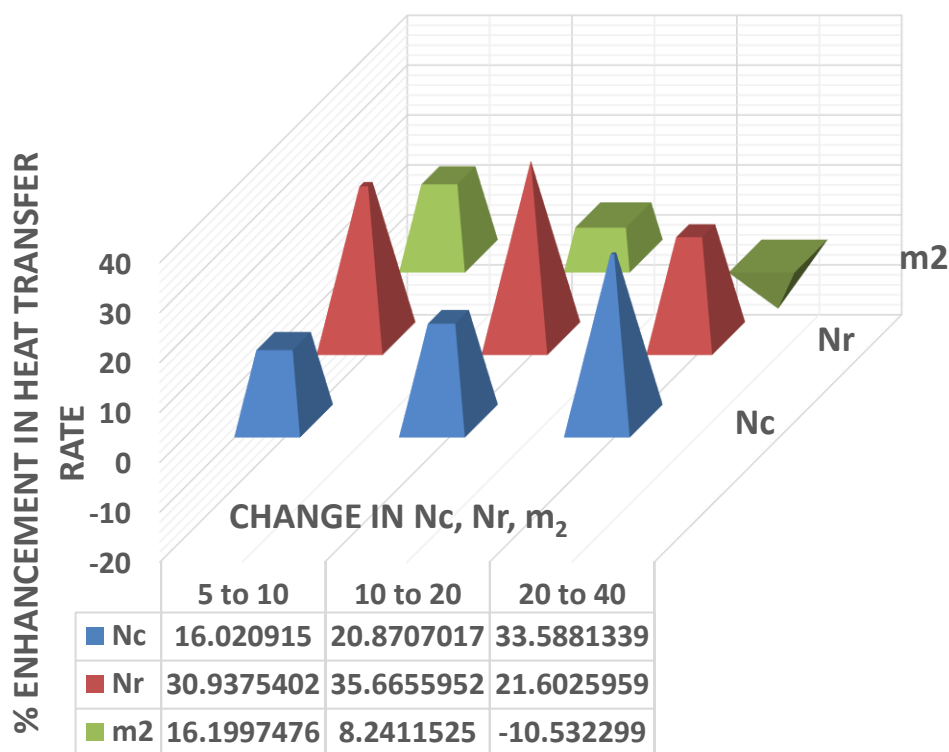| CHANGE IN Nc, Nr, m_2	5 to 10	10 to 20	20 to 40
Nc	16.020915	20.8707017	33.5881339
Nr	30.9375402	35.6655952	21.6025959
m2	16.1997476	8.2411525	-10.532299

Fig. 12. Percentage enhancement in the heat transfer rate of *IHNFHSM* for two-fold rise in Nc, Nr and m_2 values

3.9 Effect of Nanoparticle Shape

A quantitative metric that describes the geometry or morphology of nanoparticles is the shape factor. It provides an insight to the shape characteristics of nanoparticles that can vary depending on the material qualities and synthesis technique employed. Table 4 shows the shape factor for various shapes of nanoparticle. The effect of this parameter by changing the shapes of the alumina and SiC nanoparticles on the thermal profile, for different values of Nc are indicated in Figure 13 to Figure 19. From the simulation results obtained, it was observed that for a given value of Nc, the convective tip fin temperature distribution enhanced with an increase in the values of shape factor, thus

impacting the rate of heat transmission. The dimensionless temperatures at the tip of the fin (X = 1) for various combination of shapes of nanoparticle and various convective parameter values are depicted in Figure 20 to Figure 22. By changing the combination of shapes of the alumina and SiC nanoparticles from lamina – spherical to lamina – lamina, the dimensionless temperature at the fin tip increased by 12.16% for Nc = 1, clearly proving its outperformance over the other combinations. The effect of lamina shaped Alumina with different shapes of Silicon carbide nanoparticles on the fin temperature distribution for various values of Nc is shown in Figure 16 and in particular lamina – lamina combination in Figure 17.

Table 4
Shape factor of the nanoparticles [31]

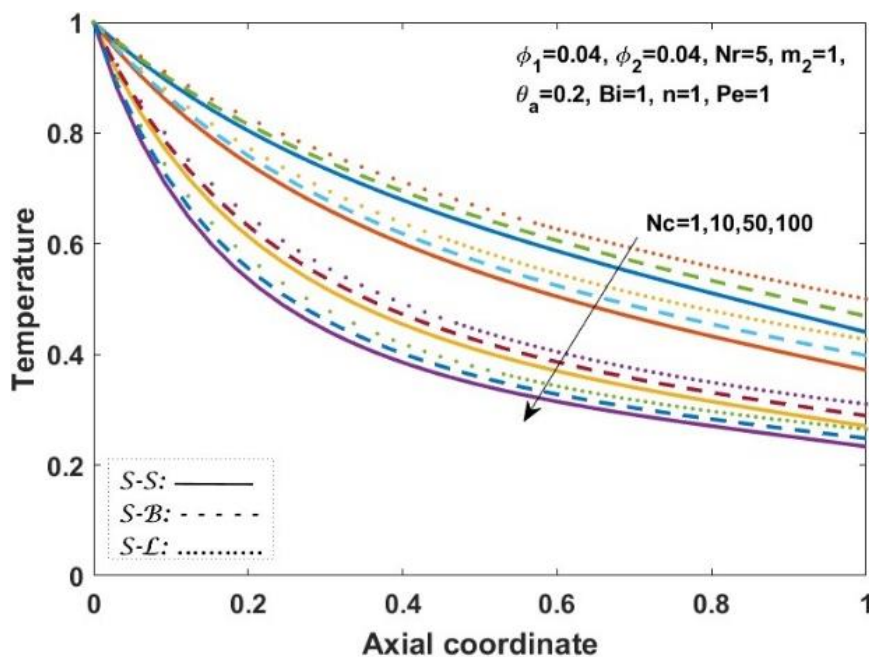| Nanoparticles Type	Shape	Shape factor, α
Spherical		3
Blade		8.9
Lamina		16.2

Fig. 13. Temperature profile of convective fin tip for spherical shaped alumina with various shapes of Silicon carbide nanoparticles in a hybrid nanofluid for various values of Nc
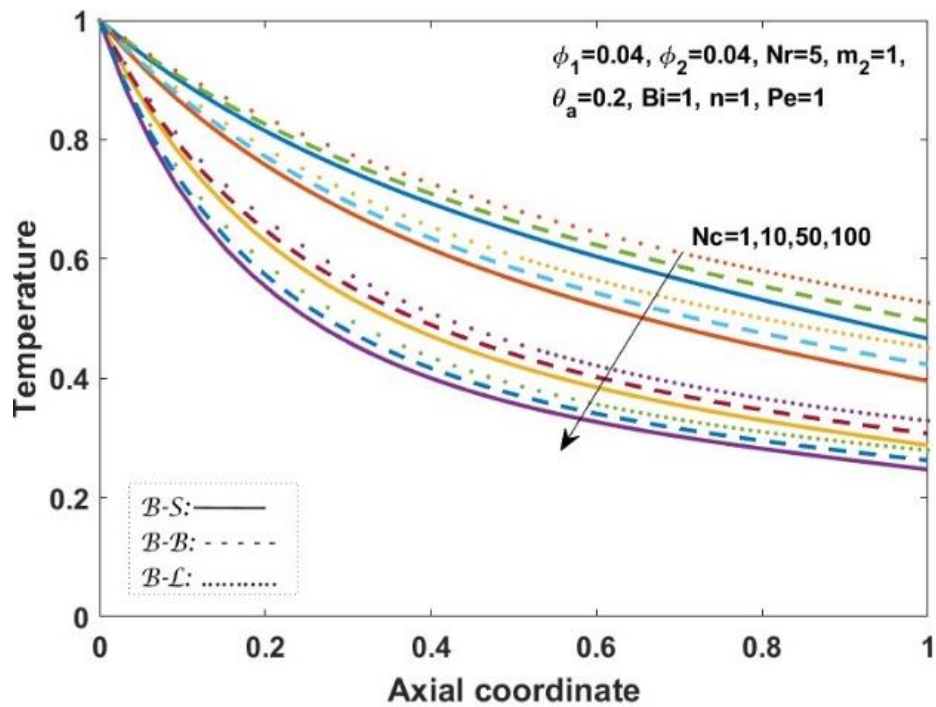
Fig. 14. Temperature profile of convective fin tip with blade shaped alumina and various shapes of Silicon carbide nanoparticles in a hybrid nanofluid for various values of Nc
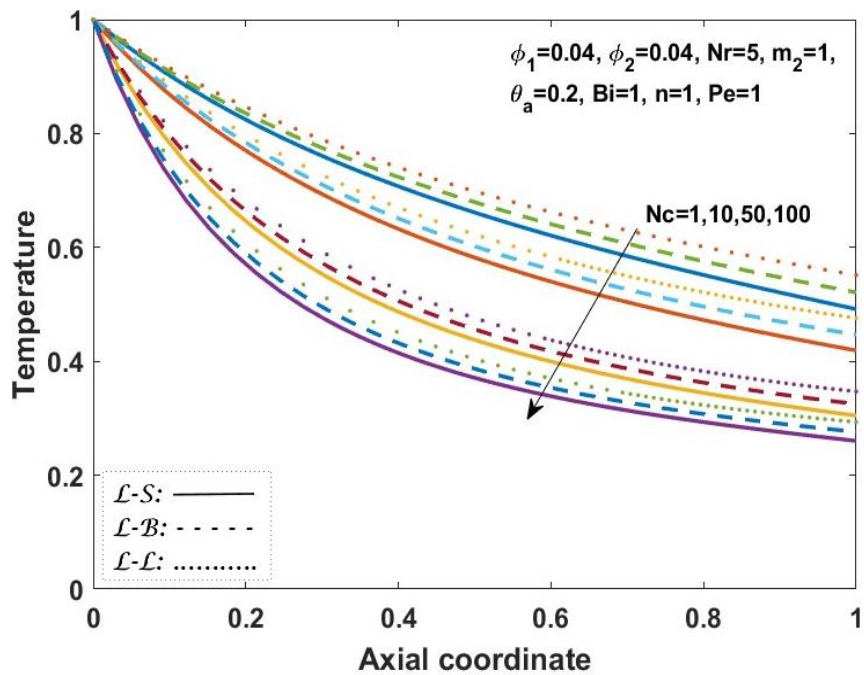

Fig. 15. Temperature profile of convective fin tip with lamina shaped alumina and various shapes of Silicon carbide nanoparticles in a hybrid nanofluid for various values of Nc
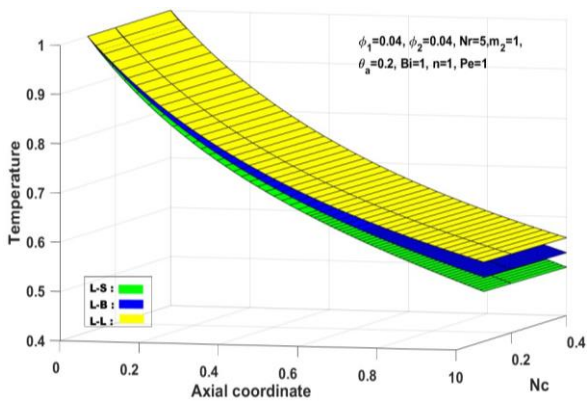
Fig. 16. Convective fin tip temperature profile with lamina shaped Al_2O_3 and different shapes of SiC nanoparticles in a hybrid nanofluid for Nc = 0.2, 0.4 and 0.6

Fig. 17. Convective fin tip temperature profile with lamina − lamina shape combination of Al_2O_3− SiC nanoparticles in a hybrid nanofluid for Nc = 0.1, 0.2, 0.3, 0.4 and 0.5

Fig. 18. Convective fin tip temperature profile with spherical shaped Al_2O_3 and different shapes of SiC nanoparticles in a hybrid nanofluid for Nc = 0.2, 0.4 and 0.6
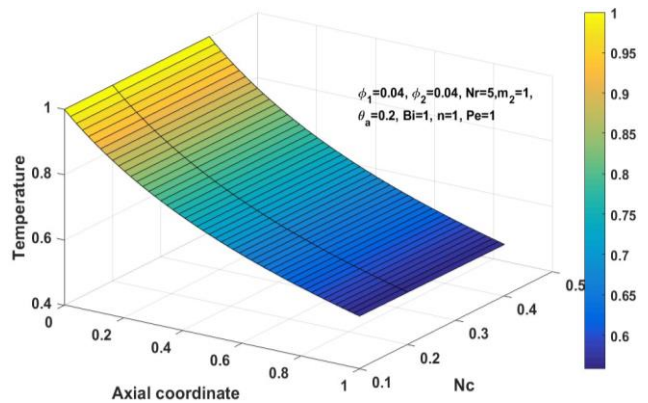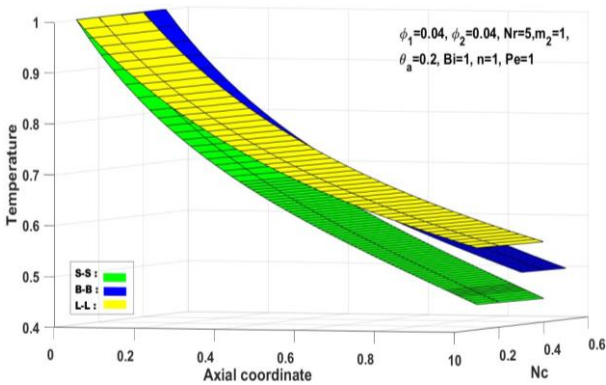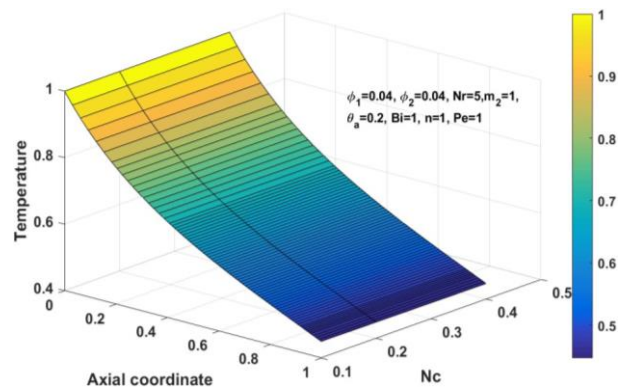

Fig. 19. Convective fin tip temperature profile with spherical − spherical shape combination of Al_2O_3− SiC nanoparticles in a hybrid nanofluid for Nc = 0.1, 0.2, 0.3, 0.4 and 0.5

	1	10	50	100
Spherical - Spherical	0.4402	0.3714	0.2704	0.2334
Sperical - Blade	0.469	0.3979	0.2893	0.2482
Sperical - Lamina	0.4998	0.4267	0.3102	0.2646

Fig. 20. Impact of Spherical shape alumina with various shapes of Silicon Carbide nanoparticle on convective tip fin temperature at X = 1 for Nc = 1, 10, 50, 100

	1	10	50	100
Blade - Spherical	0.4662	0.3953	0.2874	0.2468
Blade - Blade	0.4953	0.4225	0.3071	0.2622
Blade - Lamina	0.5261	0.4516	0.3286	0.279

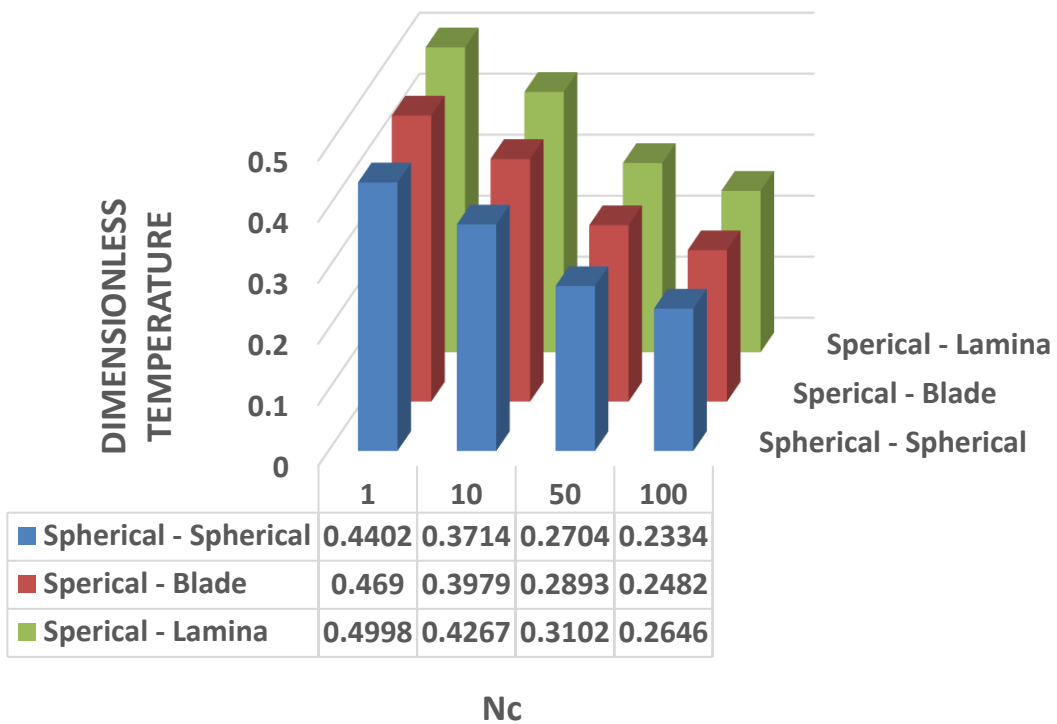**Fig. 21.** Impact of Blade shape alumina with various shapes of Silicon Carbide nanoparticle on convective tip fin temperature at X = 1 for Nc = 1, 10, 50, 100
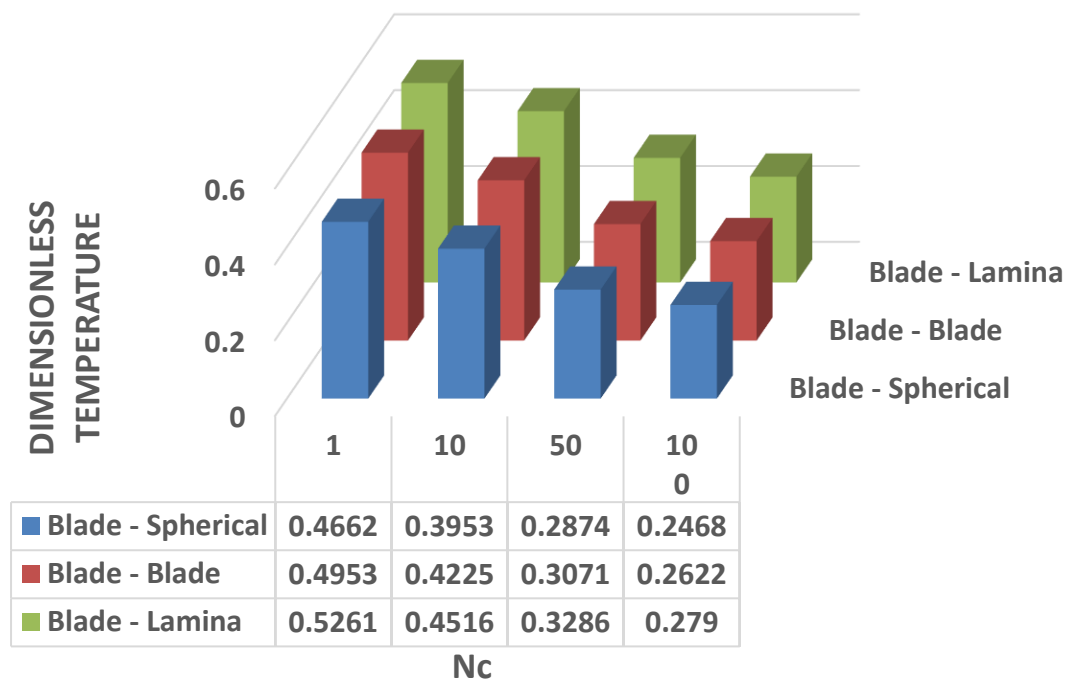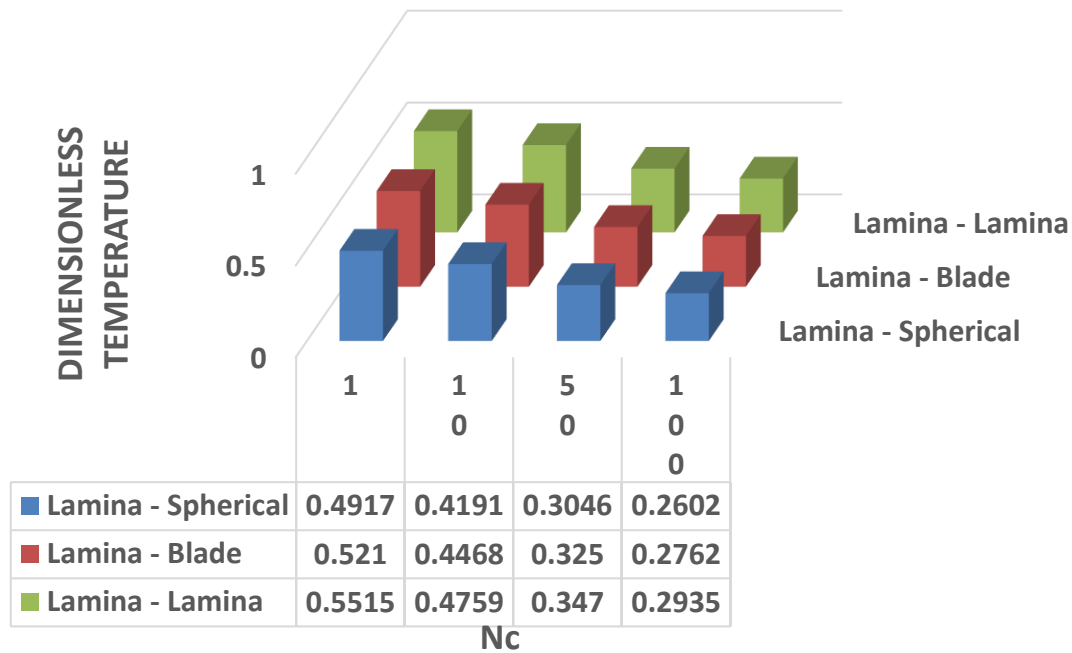
Fig. 22. Impact of Lamina shape alumina with various shapes of Silicon Carbide nanoparticle on convective tip fin temperature at X = 1 for Nc = 1, 10, 50, 100

4. Conclusions

The analysis examines the heat transfer rate of a wet penetrable rectangular moving fin in a shape dependent Al_2O_3-SiC/H_2O hybrid nanofluid subjected to boundary conditions. The findings of this study demonstrate the use of Al_2O_3-SiC combination in a base fluid H_2O for an efficient heat transfer application, by optimizing the influence of different thermal parameters and nanoparticle shape in a moving wet porous rectangular fin. Fins are efficient and simple structures used to enhance rate of heat flow from surface to the fluid. The performance of a moving fin to transmit the heat in a hybrid nanofluid is largely dependent on the flow characteristics of the hybrid nanofluid, including its heat capacity, thermal conductivity, flow resistance and convective heat flow. In this study, the dimensionless temperature profile and heat transfer rate are the important parameters in assessing the thermal performance of heat sink.

i.   Heat radiation and natural convection have a significant impact on the fin cooling. An increase in convective, radiative and wet porous parameters results in an enhanced heat transfer rate.

ii. The convective, radiative and wet porous parameters can be adjusted to optimize the thermal performance of *IHNFPHS* model.

iii. Improvement in the rate of heat transfer with Peclet number reduction, as it enhances the interface with the surrounding.

iv. An appreciable amount of enhancement in the temperature distribution of the fin was observed by changing the shapes of Al_2O_3-SiC dispersed in H_2O compared to other hybrid nanofluids found in the literature, with the increase in value of convective parameter. The lamina-shaped particles outperformed the blade and spherical-shaped nanoparticles due to their superior surface area to volume ratio, enhancing the thermal conduction and convective heat transfer coefficient of the nanofluid suggesting their potential for improving cooling systems in various applications.

The proposed model can be incorporated into an electronic cooling system to effectively enhance the heat transfer rate and reduce the power consumption of electronic chip.

Further studies can be carried out:

i. To improve the heat transfer rate by changing the nanoparticle combination based on thermal conductivity, as well as changing the shape and concentration of the nanoparticles. The study may require simulation to identify the efficient hybrid nanofluid formulation and experimental verification.

ii. To examine the dynamic behavior of the fins with different geometries placed in hybrid nanofluids under various operating conditions. The investigation can facilitate a more efficient as well as durable heat transfer system.

References

[1] Sharqawy, Mostafa H., and Syed M. Zubair. "Efficiency and optimization of straight fins with combined heat and mass transfer-an analytical solution." *Applied Thermal Engineering* 28, no. 17-18 (2008): 2279-2288. https://doi.org/10.1016/j.applthermaleng.2008.01.003

[2] Din, Zia Ud, Amir Ali, Zareen A. Khan, and Gul Zaman. "Investigation of moving trapezoidal and exponential fins with multiple nonlinearities." *Ain Shams Engineering Journal* 14, no. 5 (2023): 101959. https://doi.org/10.1016/j.asej.2022.101959

[3] Turkyilmazoglu, Mustafa. "Thermal management of parabolic pin fin subjected to a uniform oncoming airflow: optimum fin dimensions." *Journal of Thermal Analysis and Calorimetry* 143, no. 5 (2021): 3731-3739. https://doi.org/10.1007/s10973-020-10382-x

[4] Kezzar, Mohamed, Ismail Tabet, and Mohamed R. Eid. "A new analytical solution of longitudinal fin with variable heat generation and thermal conductivity using DRA." *The European Physical Journal Plus* 135, no. 1 (2020): 1-15. https://doi.org/10.1140/epjp/s13360-020-00206-0

[5] Hosseinzadeh, Kh, A. R. Mogharrebi, A. Asadi, M. Paikar, and D. D. Ganji. "Effect of fin and hybrid nano-particles on solid process in hexagonal triplex latent heat thermal energy storage system." *Journal of Molecular Liquids* 300 (2020): 112347. https://doi.org/10.1016/j.molliq.2019.112347

[6] Elbahjaoui, Radouane, and Hamid El Qarnia. "Transient behavior analysis of the melting of nanoparticle-enhanced phase change material inside a rectangular latent heat storage unit." *Applied Thermal Engineering* 112 (2017): 720-738. https://doi.org/10.1016/j.applthermaleng.2016.10.115

[7] Ahmad, Ashfaq, Muhammad Sulaiman, Ahmad Alhindi, and Abdulah Jeza Aljohani. "Analysis of temperature profiles in longitudinal fin designs by a novel neuroevolutionary approach." *IEEE Access* 8 (2020): 113285-113308. https://doi.org/10.1109/ACCESS.2020.3003253

[8] Ali, Abdullah Masoud, Matteo Angelino, and Aldo Rona. "Numerical analysis on the thermal performance of microchannel heat sinks with Al_2O_3 nanofluid and various fins." *Applied Thermal Engineering* 198 (2021): 117458. https://doi.org/10.1016/j.applthermaleng.2021.117458

[9] Syed, K. S., Muhammad Ishaq, Zafar Iqbal, and Ahmad Hassan. "Numerical study of an innovative design of a finned double-pipe heat exchanger with variable fin-tip thickness." *Energy Conversion and Management* 98 (2015): 69-80. https://doi.org/10.1016/j.enconman.2015.03.038

[10] Mukeshkumar, P. C., and Arun Kumar. "Numerical study on the performance of Al_2O_3/water nanofluids as a coolant in the fin channel heat sink for an electronic device cooling." *Materials Today: Proceedings* (2023).

[11] Vinoth, R., B. Sachuthananthan, A. Vadivel, S. Balakrishnan, and A. Gnana Sagaya Raj. "Heat transfer enhancement in oblique finned curved microchannel using hybrid nanofluid." *International Journal of Thermal Sciences* 183 (2023): 107848. https://doi.org/10.1016/j.ijthermalsci.2022.107848

[12] Sowmya, G., B. J. Gireesha, and Hamza Berrehal. "An unsteady thermal investigation of a wetted longitudinal porous fin of different profiles." *Journal of Thermal Analysis and Calorimetry* 143 (2021): 2463-2474. https://doi.org/10.1007/s10973-020-09963-7

[13] Nabati, M., M. Jalalvand, and S. Taherifar. "Sinc collocation approach through thermal analysis of porous fin with magnetic field." *Journal of Thermal Analysis and Calorimetry* 144 (2021): 2145-2158. https://doi.org/10.1007/s10973-020-09923-1

[14] Atouei, S. A., Kh Hosseinzadeh, M. Hatami, Seiyed E. Ghasemi, S. A. R. Sahebi, and D. D. Ganji. "Heat transfer study on convective-radiative semi-spherical fins with temperature-dependent properties and heat generation using efficient computational methods." *Applied Thermal Engineering* 89 (2015): 299-305. https://doi.org/10.1016/j.applthermaleng.2015.05.084

[15] Sajid, Muhammad Usman, and Hafiz Muhammad Ali. "Thermal conductivity of hybrid nanofluids: a critical review." *International Journal of Heat and Mass Transfer* 126 (2018): 211-234. https://doi.org/10.1016/j.ijheatmasstransfer.2018.05.021

[16] Yang, Liu, Weikai Ji, Mao Mao, and Jia-nan Huang. "An updated review on the properties, fabrication and application of hybrid-nanofluids along with their environmental effects." *Journal of Cleaner Production* 257 (2020): 120408. https://doi.org/10.1016/j.jclepro.2020.120408

[17] Das, Pritam Kumar. "A review based on the effect and mechanism of thermal conductivity of normal nanofluids and hybrid nanofluids." *Journal of Molecular Liquids* 240 (2017): 420-446. https://doi.org/10.1016/j.molliq.2017.05.071

[18] Babar, Hamza, and Hafiz Muhammad Ali. "Towards hybrid nanofluids: preparation, thermophysical properties, applications, and challenges." *Journal of Molecular Liquids* 281 (2019): 598-633. https://doi.org/10.1016/j.molliq.2019.02.102

[19] Ghadikolaei, S. S., M. Yassari, H. Sadeghi, Kh Hosseinzadeh, and D. D. Ganji. "Investigation on thermophysical properties of Tio$_2$-Cu/H$_2$O hybrid nanofluid transport dependent on shape factor in MHD stagnation point flow." *Powder technology* 322 (2017): 428-438. https://doi.org/10.1016/j.powtec.2017.09.006

[20] Gireesha, Bijjanal Jayanna, G. Sowmya, M. Ijaz Khan, and Hakan F. Öztop. "Flow of hybrid nanofluid across a permeable longitudinal moving fin along with thermal radiation and natural convection." *Computer Methods and Programs in Biomedicine* 185 (2020): 105166. https://doi.org/10.1016/j.cmpb.2019.105166

[21] Hosseinzadeh, Kh, A. Asadi, A. R. Mogharrebi, M. Ermia Azari, and D. D. Ganji. "Investigation of mixture fluid suspended by hybrid nanoparticles over vertical cylinder by considering shape factor effect." *Journal of Thermal Analysis and Calorimetry* 143, no. 2 (2021): 1081-1095. https://doi.org/10.1007/s10973-020-09347-x

[22] Keerthi, M. L., B. J. Gireesha, and G. Sowmya. "Numerical investigation of efficiency of fully wet porous convective-radiative moving radial fin in the presence of shape-dependent hybrid nanofluid." *International Communications in Heat and Mass Transfer* 138 (2022): 106341. https://doi.org/10.1016/j.icheatmasstransfer.2022.106341

[23] Talbi, Nabil, Mohamed Kezzar, Manuel Malaver, Ismail Tabet, Mohamed Rafik Sari, Abderrezak Metatla, and Mohamed R. Eid. "Increment of heat transfer by graphene-oxide and molybdenum-disulfide nanoparticles in ethylene glycol solution as working nanofluid in penetrable moveable longitudinal fin." *Waves in Random and Complex Media* (2022): 1-23. https://doi.org/10.1080/17455030.2022.2026527

[24] AlBaidani, Mashael M., Nidhish Kumar Mishra, Mohammad Mahtab Alam, Sayed M. Eldin, Asla A. AL-Zahrani, and Ali Akgul. "Numerical analysis of magneto-radiated annular fin natural-convective heat transfer performance using advanced ternary nanofluid considering shape factors with heating source." *Case Studies in Thermal Engineering* 44 (2023): 102825. https://doi.org/10.1016/j.csite.2023.102825

[25] Esfahani, Navid Nasajpour, Davood Toghraie, and Masoud Afrand. "A new correlation for predicting the thermal conductivity of ZnO-Ag (50%-50%)/water hybrid nanofluid: an experimental study." *Powder Technology* 323 (2018): 367-373. https://doi.org/10.1016/j.powtec.2017.10.025

[26] Aparna, Z., Monisha Michael, S. K. Pabi, and S. Ghosh. "Thermal conductivity of aqueous Al$_2$O$_3$/Ag hybrid nanofluid at different temperatures and volume concentrations: an experimental investigation and development of new correlation function." *Powder Technology* 343 (2019): 714-722. https://doi.org/10.1016/j.powtec.2018.11.096

[27] Huminic, Gabriela, Angel Huminic, Florian Dumitrache, Claudiu Fleacă, and Ion Morjan. "Study of the thermal conductivity of hybrid nanofluids: Recent research and experimental study." *Powder Technology* 367 (2020): 347-357. https://doi.org/10.1016/j.powtec.2020.03.052

[28] Scott, T. O., D. R. E. Ewim, and A. C. Eloka-Eboka. "Experimental study on the influence of volume concentration on natural convection heat transfer with Al$_2$O$_3$-MWCNT/water hybrid nanofluids." *Materials Today: Proceedings* (2023). https://doi.org/10.1016/j.matpr.2023.07.290

[29] Al-Hossainy, Ahmed F., and Mohamed R. Eid. "Combined experimental thin films, TDDFT-DFT theoretical method, and spin effect on [PEG-H$_2$O/ZrO^{2+} MgO] h hybrid nanofluid flow with higher chemical rate." *Surfaces and Interfaces* 23 (2021): 100971. https://doi.org/10.1016/j.surfin.2021.100971

[30] Venkatesan, Sorakka Ponnappan, B. Keshava Kalyan, G. Gopinath, M. Purusothaman, and J. Hemanandh. "Study of the performance of a coolant mixed with an Al$_2$O$_3$/SiC nanomaterial in an engine radiator." *Environmental Quality Management* 33, no. 1 (2023): 53-59. https://doi.org/10.1002/tqem.21950

[31] Akbar, Asia Ali, N. Ameer Ahammad, Aziz Ullah Awan, Ahmed Kadhim Hussein, Fehmi Gamaoun, ElSayed M. Tag-ElDin, and Bagh Ali. "Insight into the role of nanoparticles shape factors and diameter on the dynamics of rotating water-based fluid." *Nanomaterials* 12, no. 16 (2022): 2801. https://doi.org/10.3390/nano12162801

[32] Alkasasbeh, Hamzeh T. "Numerical solution of heat transfer flow of casson hybrid nanofluid over vertical stretching sheet with magnetic field effect." *CFD Letters* 14, no. 3 (2022): 39-52. https://doi.org/10.37934/cfdl.14.3.3952

[33] Saupi, Suhaila, Aniza Abd Ghani, Norihan Md Arifin, Haliza Rosali, and Nur Syahirah Wahid. "An Exact Solution of MHD Hybrid Nanofluid over a Stretching Surface Embedded in Porous Medium in the Presence of Thermal Radiation and Slip with Suction." *CFD Letters* 15, no. 5 (2023): 74-85. https://doi.org/10.37934/cfdl.15.5.7485

[34] Muhammad, Nura Mu'az, and Nor Azwadi Che Sidik. "Applications of nanofluids and various minichannel configurations for heat transfer improvement: A review of numerical study." *Journal of Advanced Research in Fluid Mechanics and Thermal Sciences* 46, no. 1 (2018): 49-61.

[35] Elfaghi, Abdulhafid M. A., Alhadi A. Abosbaia, Munir F. A. Alkbir, and Abdoulhdi A. B. Omran. "CFD Simulation of Forced Convection Heat Transfer Enhancement in Pipe Using Al₂O₃/Water Nanofluid." *Journal of Advanced Research in Micro and Nano Engineering* 7, no. 1 (2022): 8-13.

[36] Sidik, N. A. Che, and O. Adnan Alawi. "Computational investigations on heat transfer enhancement using nanorefrigerants." *Journal of Advanced Research Design* 1, no. 1 (2014): 35-41.